Brief communication

MOLECULAR METABOLISM

Rapid glutamate release in the mediobasal hypothalamus accompanies feeding and is exaggerated by an obesogenic food

Stephan J. Guyenet [1], Miles E. Matsen [1], Gregory J. Morton [1], Karl J. Kaiyala [2], Michael W. Schwartz [1,*]

ABSTRACT

The mediobasal hypothalamus (MBH) plays a central role in the regulation of food intake and energy balance. Although the excitatory neurotransmitter glutamate is implicated in energy balance regulation by the MBH, the hypothesis that feeding elicits local glutamate release remains untested. To test this hypothesis, we employed a glutamate biosensor that measures glutamate concentrations at 1-s intervals in conscious, freely behaving rats. Results indicate that feeding is associated with an increase of MBH glutamate concentration that occurs within 1–2 s of oral contact with a food pellet, and the glutamate response to a palatable high-fat pellet is greatly exaggerated relative to chow. In contrast, glutamate responses were not observed during water ingestion or other observed behaviors. These findings indicate that feeding is associated with rapid release of glutamate in the MBH, that this release is exaggerated with an obesogenic food, and that this response is likely stimulated by orosensory factors.

Keywords Hypothalamus; Glutamate; Food intake; Arcuate nucleus; High-fat diet

1. INTRODUCTION

The mediobasal hypothalamus (MBH) is a key site for the homeostatic control of energy balance and glucose homeostasis in response to circulating signals of energy status [1,2]. While much is known regarding the control of MBH neurons by humoral inputs, far less is known about the role of local neurotransmitters. The amino acid glutamate is the dominant excitatory neurotransmitter in the central nervous system (CNS), and the hypothalamus is richly endowed with both glutamatergic terminals and receptors [3–6]. Moreover, nearly all MBH neurons can be stimulated by glutamate agonists and are silenced by glutamate antagonists [6]. While many brain regions project to the MBH [7–10], and some glutamatergic projections have been identified [10,11], a comprehensive accounting of the glutamatergic projections to this brain area and their role(s) in energy homeostasis is still awaited.

Several studies implicate hypothalamic glutamate signaling in the control of food intake. For example, increased glutamatergic signaling in the lateral hypothalamic area (LHA) potently stimulates feeding [12], and microdialysis experiments have linked LHA glutamate release to feeding bouts *in vivo* [13,14]. The hormone ghrelin reportedly increases glutamatergic synaptic input onto orexigenic agouti-related peptide (AgRP) neurons in the hypothalamic arcuate nucleus (ARC) via a mechanism antagonized by leptin, suggesting a role for glutamate in the response of energy balance circuits to circulating hormones [15]. Similarly, mice with AgRP neuron-specific deletion of NMDA receptors are characterized by reduced food intake and body fat mass [16], whereas selective impairment of glutamate release in the ventromedial hypothalamic nucleus (VMH)-specific modestly increases food intake and fat mass during purified high-fat diet (HFD) feeding [17]. An important unanswered question is whether glutamate release in the MBH is provoked by feeding-relevant stimuli, as one might expect if local glutamatergic signaling plays a role in feeding and energy homeostasis.

2. MATERIALS AND METHODS

2.1. Animals

All procedures were performed in accordance with National Institutes of Health Guidelines for the Care and Use of Animals and were approved by the Animal Care and Use Committee at the University of Washington. Weight-matched male Wistar rats (300–350 g; Harlan Laboratories, Indianapolis, IN) were housed individually in a specific pathogen-free environment, maintained in a temperature-controlled room with a 12 h light/dark cycle (light 6 am to 6 pm), and provided with *ad libitum* access to water and standard unpurified laboratory chow (PMI Nutrition International; 3.34 kcal/g) unless otherwise stated.

2.2. Guide cannula implantation

Guide cannulae and head caps (potentiostat housing) were purchased from Pinnacle Technology (Lawrence, KS). Animals maintained under isoflurane anesthesia were implanted with a guide cannula per

[1]Diabetes and Obesity Center of Excellence, Department of Medicine, University of Washington, UW Medicine at South Lake Union, 850 Republican Street, Box 358055, Seattle, WA 98109, USA [2]School of Dentistry, Department of Oral Health Sciences, University of Washington, UW Health Sciences Building, 1959 N.E. Pacific Street, Box 357473, Seattle, WA 98195, USA

*Corresponding author. Tel.: +1 206 897 5288; fax: +1 206 897 5293. Email: guyenet@uw.edu (S.J. Guyenet), matsen18@uw.edu (M.E. Matsen), gjmorton@uw.edu (G.J. Morton), kkaiyala@uw.edu (K.J. Kaiyala), mschwart@uw.edu (M.W. Schwartz)

Received January 25, 2013 • Revision received February 2, 2013 • Accepted February 4, 2013 • Available online 11 February 2013

http://dx.doi.org/10.1016/j.molmet.2013.02.001

manufacturer specifications, targeting the hypothalamic ARC using the following stereotaxic coordinates: −2.8 mm posterior to bregma, 0.35 mm lateral (right), and −7.3 mm below the skull surface (Figure 1A). Animals were allowed to recover for 10 days prior to biosensor implantation, during which time they were habituated to experimental protocol conditions, including three exposures to a HFD pellet (Research Diets D12492; 5.24 kcal/g, 60% kcal from fat).

2.3. Biosensor calibration and implantation

Biosensors, wireless potentiostats, wireless base stations, and recording/processing software were purchased from Pinnacle Technology (Lawrence, KS). Biosensors detect glutamate using a glutamate oxidase outer layer, and a selectively permeable membrane barrier that excludes other electron donors such as ascorbate (Figure 1B). The potentiostat wirelessly communicates with a computer-connected base station, and current readings are visualized and recorded using Pinnacle Acquisition Laboratory software. Prior to implantation, each biosensor was pre-calibrated by immersion in 37 °C PBS (150 mM NaCl, 8.7 mM Na_2HPO_4, 16 mM KH_2PO_4, pH 7.4) and adding three boluses of L-glutamic acid (+10 μM total glutamate increment for each addition) and one bolus of the electron donor ascorbic acid to verify specificity (+250 μM ascorbate increment) (Figure 1B).

On the experimental day, live, conscious animals were implanted with the biosensor, following pre-calibration (well tolerated in habituated animals). Each biosensor projects 3.1 mm beyond the end of the guide cannula, and the 1 mm sensing cavity spans the ARC and medial VMH (Figure 1A).

2.4. Recording and placement analysis

On the day of recording, animals were placed in clear animal housing enclosures (Instech Solomon) at 9 am (early light cycle), with bedding and water but without food (Figure 1C). Animals were then allowed to acclimate until 1 pm before implantation with the biosensor as described earlier. Following the implantation, current trace recording was initiated, and the biosensor was allowed to equilibrate until dark cycle onset at 6 pm.

At dark cycle onset, animals were provided with *ad libitum* access to chow and visually observed for an average of 3 h, and the time of onset and termination of all feeding and drinking bouts were recorded. In addition to standard chow, each rat was given individual HFD pellets (~2 g) 2–4 times, with a 10–30 min washout period between each. Approximately 3 h after dark cycle onset, animals were anesthetized with isoflurane and biosensors explanted. Biosensors were post-calibrated in the manner described above. The following day, animals were placed under ketamine/xylazine anesthesia and perfused with PBS followed by 4% paraformaldehyde. Brains were processed for histochemical analysis, sectioned in the coronal plane by cryostat at 25 μM and analyzed for cannula placement under a dissecting microscope. Cannula tracts were clearly visible on unstained sections.

2.5. Analysis of glutamate data

To calculate the current-to-glutamate conversion factor, linear regression analysis was applied to post-calibration data. To estimate the glutamate response to feeding and drinking, the baseline current value (calculated by averaging two 10 s periods immediately prior to and following the feeding bout) was subtracted from the mean value during the first 30 s of feeding. To estimate the glutamate response associated with randomly selected periods, we chose five random 30 s periods within the dark cycle using a random number generator (http://www.random.org), replacing any time point that was associated with a feeding or drinking period. Each selected 30 s period was quantified as above. If no increment in glutamate was observed during the selected period, the baseline value was calculated using two 10 s periods immediately prior to and following the selected 30 s period. If the randomly selected 30 s period included an increment in glutamate

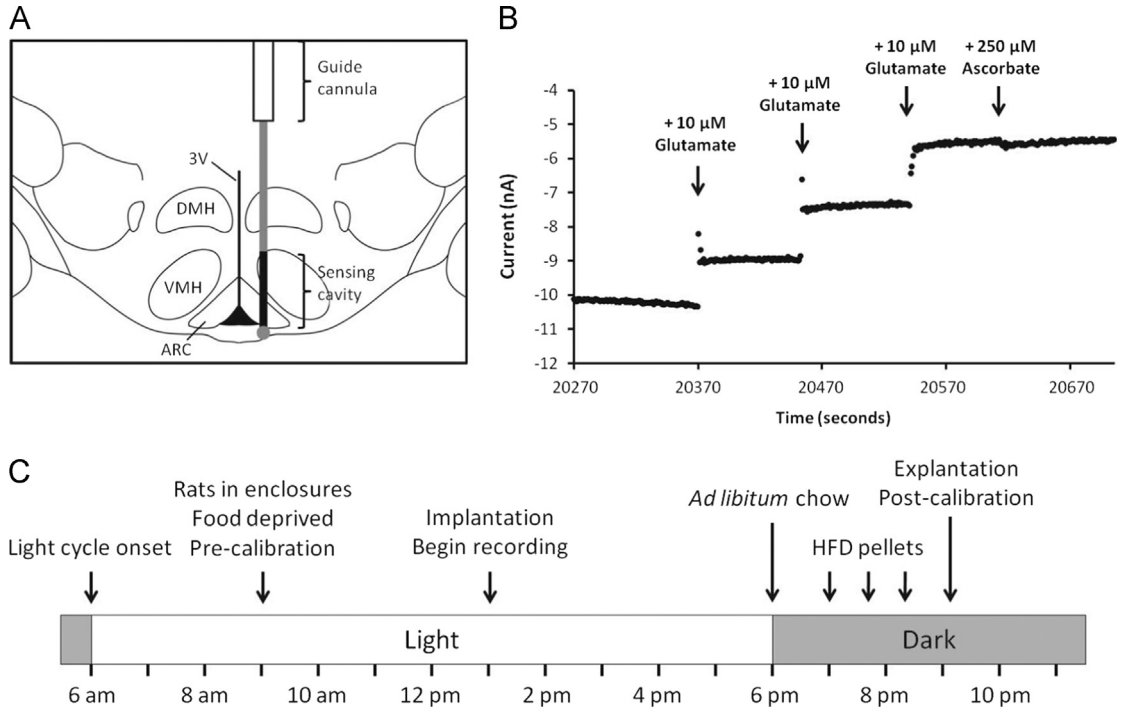

Figure 1: Biosensor targeting and calibration. (A) Scale model of the rat hypothalamus at bregma −2.8, with guide cannula and biosensor. Black area indicates 1-mm sensing cavity. (B) Representative trace of biosensor calibration with glutamate and ascorbate (a negative control). (C) Timeline of experimental procedure on the day of recording.

concentration, the increment was computed by subtracting a 10 s baseline period following return to baseline.

2.6. Statistical analysis

The sign test was used to determine whether the glutamate increment associated with feeding was significantly different from randomly selected periods. For each subject, the mean glutamate increment for all random periods and all feeding bouts was calculated. Within each subject, we determined if the difference between feeding *vs.* random sampling was positive or negative. We then determined whether this distribution of signs was significantly different from that expected by chance across the entire cohort, with each subject representing $n=1$.

To test for significant differences in glutamate increments associated with chow *vs.* HFD, the Wilcoxon signed rank test was applied. For each subject, the mean glutamate increment for all chow and HFD feeding bouts was calculated separately. Applying the Wilcoxon signed rank test to the entire cohort, we compared the magnitude of glutamate increment between chow and HFD feeding conditions, with each subject representing $n=1$.

To test for a significant association between biosensor placement and glutamate response, we employed simple linear regression including all subjects for which localization data are available.

3. RESULTS

3.1. Feeding is associated with rapid increases of MBH extracellular glutamate in freely behaving rats

During a 3-h period of recording and observation beginning at dark cycle onset, biosensor-implanted rats were given *ad libitum* access to standard rodent chow, and were also intermittently provided with pellets of HFD (Figure 1C). In nine of 11 animals, feeding (either chow or HFD) was associated with a rapid increase of MBH extracellular glutamate concentration. This was detectable within 1–2 s of oral contact and typically remained elevated for the duration of the feeding bout (Figs. 2 and 3B). After completion of the feeding bout, the concentration of extracellular glutamate returned to baseline within 1–15 s, depending on the magnitude of the feeding-associated increment (Figure 2). In all instances where HFD feeding was accompanied by an increase of MBH glutamate ($n=9$), the increase was clearly evident within 1–2 s of oral contact with the pellet (Figs. 2 and 3C), and the maximal glutamate increment also occurred within 1–2 s in seven of nine subjects, with the remaining two occurring within 7 s. Chow feeding was also typically associated with an increase of MBH glutamate within 1–2 s, although this response smaller than with HFD and was observed in only five of the seven animals that exhibited a clear increase of MBH glutamate in response to chow feeding (Figs. 2 and 3C). Extracellular glutamate concentration fluctuated rapidly during feeding in both chow and HFD conditions (Figure 2).

In contrast, water consumption was not associated with increased extracellular glutamate concentrations (Figure 3C), nor was grooming, locomotion or other behaviors (data not shown). Nevertheless, transient increases of glutamate concentration were observed that were not associated with any observed behavior, raising the possibility that the association between feeding and extracellular glutamate could have arisen by chance. To test this hypothesis, we quantified five randomly selected 30-s periods from the biosensor trace of each rat. We then compared these values with the 30-s average glutamate increment during feeding behavior (chow and HFD combined; Figure 3A). In every subject, feeding was associated with a larger average 30-s glutamate

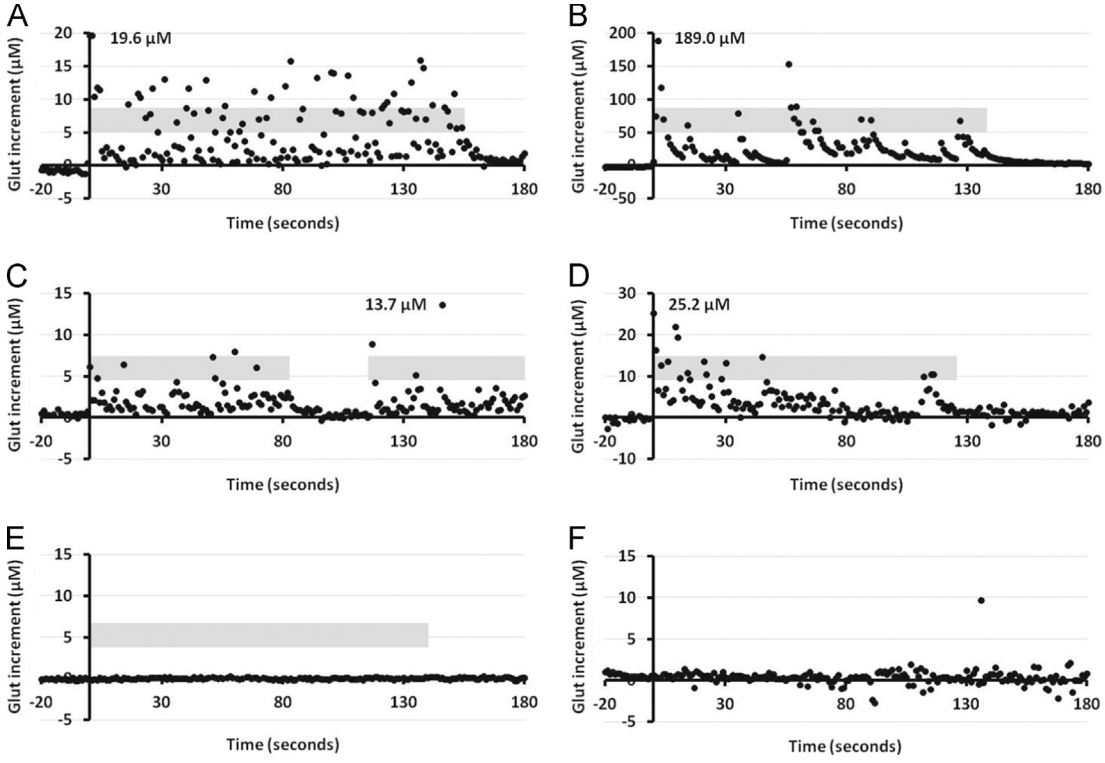

Figure 2: Representative MBH glutamate traces during chow or HFD feeding. Each point represents 1-s. Feeding begins at time 0 and duration is denoted by the gray bar. Maximum glutamate increment is indicated. (A, C, and E) Representative traces of high response, moderate response, and lack of response to chow feeding, respectively. (B, D) Representative traces of high response and moderate response to HFD feeding, respectively (note difference in *y*-axis scale between panels). (F) Representative trace of a randomly selected non-feeding period in a rat that exhibited increased MBH glutamate with food intake.

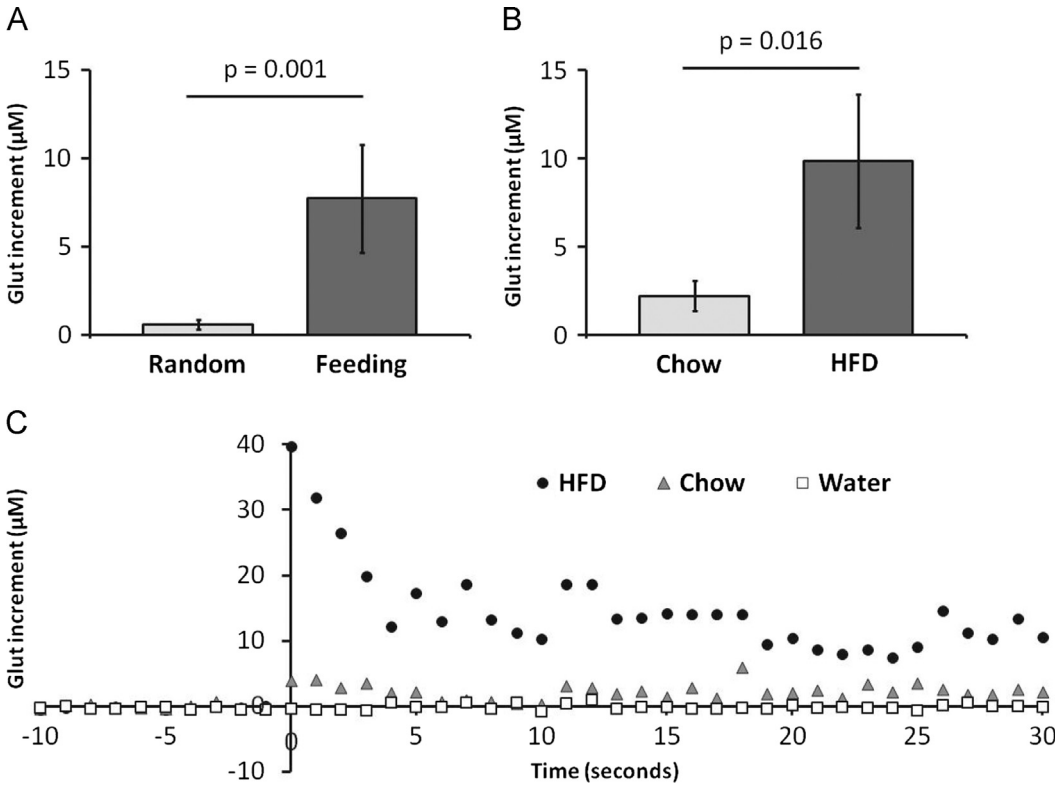

Figure 3: Average MBH glutamate during HFD feeding, chow feeding, water consumption, and randomly selected periods. (A) 30 s average glutamate increment for feeding (HFD and chow) *vs.* randomly selected periods ($n=11$ rats). *p*-Value reflects sign test. (B) 30 s average glutamate increment for chow *vs.* HFD ($n=11$ rats). *p*-Value reflects Wilcoxon rank sum test. (C) Average glutamate trace for HFD feeding, chow feeding, and water consumption in rats where biosensor entered the ARC ($n=6$, 5, 5 rats; $n=20$, 12, six feeding bouts, respectively). All error bars indicate SEM.

increment than was observed in randomly quantified 30-s periods, such that the mean glutamate increment was significantly higher during feeding than during randomly selected periods ($n=11$, $p=0.001$; sign test). Restricting the analysis to the 6 subjects in which the probe was found to have entered the ARC as intended, the feeding-associated glutamate increment remained significantly higher than expected by chance ($n=6$, $p=0.03$; sign test). Therefore, feeding is associated with a rapid increase of extracellular glutamate concentration in the MBH.

3.2. Extracellular glutamate release is higher during HFD than chow feeding

Having established an association between food consumption and increased extracellular glutamate concentration in the MBH, we next determined whether this response differed between HFD and chow. Across the entire cohort, much higher MBH glutamate concentrations were observed during HFD *vs.* chow feeding (Figs. 2 and 3). The 30-s average glutamate increment was 9.8 μM for HFD, 2.2 μM for chow, 0.0 μM for water intake, and 0.6 μM for randomly selected periods (Figure 3A and B). During the first second of feeding, differences in the average glutamate increment were more pronounced, being 39.8 μM for HFD, 4.0 μM for chow, and −0.3 μM for water, with values that subsequently declined over the course of feeding (Figure 3C). Among all nine subjects showing a clear glutamate response to HFD, four showed an average 30-s concentration >10 μM, two were between 1 and 10 μM, and three were <1 μM. Among seven subjects showing a clear glutamate response to chow feeding, four showed an average 30-s concentration between 1 and 10 μM, and three were <1 μM. Peak glutamate increments in excess of 180 μM were observed during HFD feeding in two rats, and these peaks lasted no longer than 1 s (Figure 2B). Animals with robust glutamate responses during chow feeding invariably displayed robust responses to HFD.

To test for differences in magnitude of MBH glutamate responses to feeding chow *vs.* HFD, we compared average 30-s glutamate increments during the two conditions (Figure 3B). Considering the cohort as a whole, HFD feeding was associated with a significantly greater glutamate increment than chow feeding ($n=11$, $p=0.016$; Wilcoxon signed rank test). A similar trend was observed in the subset of animals in which the probe shown to have entered the ARC as intended, although the difference in glutamate increment did not achieve statistical significance, despite being consistent among all subjects ($n=5$, $p=0.063$; Wilcoxon signed rank test). Together, these data strongly suggest that the effect of feeding on MBH extracellular glutamate concentrations is exaggerated during HFD feeding relative to chow.

3.3. Impact of biosensor placement on response strength

Variation in probe placement, owing to unavoidable technical issues (including the large diameter of the guide cannula relative to the probe (0.7 mm *vs.* 0.2 mm) and the flexibility of the probe), allowed us to assess the relationship between probe location and glutamate response. We found that placement distance from the ARC in all three dimensions correlated inversely with the magnitude of the feeding-associated glutamate increment (Figure 4A–C). Variation in the lateral dimension explained a larger proportion of the variation in feeding response ($R^2=0.17$) than the other two dimensions, as predicted given that ARC placement is more sensitive to variation in the lateral than the rostrocaudal dimension. To quantify these effects in aggregate, we created a composite score that de-emphasized the influence of variation in the rostrocaudal dimension by 50%. This

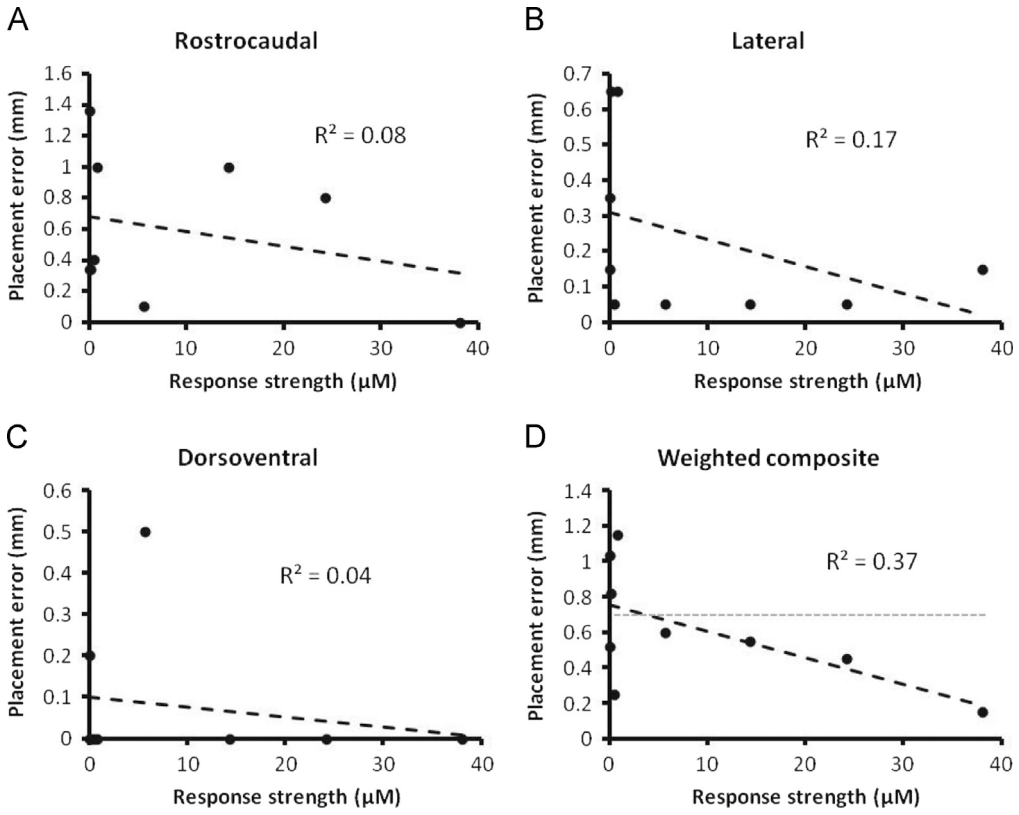

Figure 4: Association between biosensor placement error and 30 s average glutamate response to HFD feeding ($n=9$). (A) rostrocaudal error; (B) lateral error; (C) dorsoventral error. (D) Composite error score (rostrocaudal dimension weighted by a factor of 0.5), correlation $p=0.08$. The gray dashed line at 0.7 mm indicates the error value below which all biosensors successfully entered the ARC, and above which none entered the ARC.

composite error score explained 37% of the variation in feeding-associated glutamate release between subjects (Figure 4D); however the association did not reach statistical significance ($p=0.08$; linear regression). At a value of 0.7, the composite error score differentiates between subjects in which the probe entered the ARC and subjects in which it did not (Figure 4D), and in each of the three subjects in which the probe did not enter the ARC, the MBH glutamate response to feeding was small or absent. By comparison, a glutatmate response to feeding was detected in five of six—and robust in four of six—subjects in which the probe did enter the ARC (Figure 4D). Among the two animals with no detectable glutamate response to HFD feeding, the biosensor was placed in the ARC in one, but not in the other (weighted composite error of 1.03 and 0.53 mm; Figure 4D), indicating sources of experimental variability additional to biosensor placement.

Among subjects in which the ARC was successfully targeted, the glutamate response tended to be stronger when the probe was situated near the caudal edge of, or caudal to, the VMH. In the lateral dimension, maximal glutamate responses were observed with probe placement of 0.3–0.4 mm lateral from the 3rd ventricle. By comparison, probe locations lateral to the ARC but centered in the VMH yielded much weaker glutamate responses. These findings together suggest that robust feeding-induced increases of extracellular glutamate are more likely to be detected in the ARC and/or directly above the ARC than in the medial VMH or other MBH areas, and that the caudal ARC is particularly likely to elicit robust feeding-induced glutamate release. However, more work is required to critically test this hypothesis.

4. DISCUSSION

We report the first evidence that feeding rapidly increases extracellular glutamate concentrations in the MBH, and that this response is greater during HFD than chow feeding. The highly dynamic fluctuations of MBH glutamate concentrations that we observed during feeding bouts (with distinct elevations above baseline as brief as 1 s) are compatible with rapid and coordinated glutamate release from glutamatergic terminals. These findings add to growing evidence of an important role for MBH glutamate in the control of feeding behavior [10,15,16,18].

The rapidity with which glutamate release occurs following oral contact with food (generally within 1–2 s) is suggestive of a response to sensory stimulation within the oral cavity and/or upper alimentary tract, rather than nutrient contact with the stomach/intestine or absorption into the circulation (although such factors could influence glutamate release later in the feeding bout). The finding that this glutamate release was observed with food but not water ingestion suggests further that it does not result from simple mechanical stimulation of the oral cavity or activation of the swallowing reflex, but instead may be specific to feeding.

Of particular interest is our finding that the MBH glutamate response during HFD feeding was substantially greater than that observed with chow. Specifically, average 30-s glutamate release was nearly 5-fold higher, and average release in the first second was ~10-fold higher during HFD *vs.* chow ingestion, suggesting that the MBH glutamate response to feeding is strongly influenced by sensory characteristics of the food being consumed. Our data do not allow us to determine which

specific properties of the food are responsible for differences in glutamate release. We do note, however, that MBH glutamate release was not detected prior to feeding, even as the animals smelled and inspected the food and presumably identified it as either HFD or chow. It therefore seems unlikely that MBH glutamate release is related to either olfactory stimuli or anticipation of a meal or a particular food type.

The functional consequences of the feeding-induced glutamate release into the MBH remain a matter of speculation, due in part to the fact that orexigenic and anorexigenic neuronal populations are intermingled in this area. As glutamate is a rapid neurotransmitter that acts primarily at the specific synapses where it is released, measuring global extra-synaptic glutamate does not permit the identification of the MBH circuitry involved. Nevertheless, several possibilities can be considered. One of these is that MBH glutamate release serves to inform local circuits of the impending homeostatic challenge resulting from food consumption, thereby enabling anorexigenic responses to constrain intake appropriately. This hypothesis is consistent with the observed association between the energy density of food and the magnitude of glutamate release (HFD $>$ chow $>$ water), and with published work showing that in mice, consuming an energy-dense, palatable meal rapidly increases c-fos immunoreactivity in pro-opiomelanocortin (POMC) and other ARC neurons in a leptin-independent manner [19].

Alternatively, it is possible that the glutamate release we observed reflects the activation of mesolimbic reward/hedonic circuits that project to energy balance circuits in the MBH [1,2,20]. In this scenario, MBH glutamate release may serve to activate orexigenic circuits and thereby facilitate increased consumption of a preferred food. Such a mechanism is consistent with recent evidence of a role for glutamate to activate AgRP neurons [16], and would be of particular interest in light of the hypothesis that the biologically 'defended' level of fat mass is influenced by the palatability of the diet [21,22]. We note that these two possibilities are not mutually exclusive.

The neuronal origins of glutamate released into the MBH during feeding also remain unknown. Among known sources of glutamatergic input to the ARC are neurons situated within the ARC [11] and VMH [10]. The medial VMH sends glutamatergic projections to the ARC [10], and the VMH plays an important anorexigenic role in energy balance [23]. Combined with evidence that impaired release of glutamate by VMH neurons increases susceptibility to DIO [17], it is tempting to hypothesize that VMH-to-ARC connections contribute to the feeding-associated glutamate release observed in the current study. Other glutamatergic inputs to the MBH have not been systematically investigated, however, and the primary sources of glutamate release we observed remain to be determined. Given the large number of brain regions (both hypothalamic and extra-hypothalamic) that project to the MBH [7,9], additional sources of MBH glutamate will likely be identified, and future studies are needed to determine those responsible for glutamate release during feeding.

Among several limitations of the methods used in this study is that probe insertion creates local tissue damage, and the impact of this damage on glutamate release and reuptake is unknown. In addition, the interpretation of measured levels of glutamate hinges on the assumption that the glutamate sensitivity of the sensor *in vitro* corresponds precisely to its sensitivity in tissue, an assumption that cannot be proven. Similarly, the biosensor quantifies changes in glutamate from baseline rather than the absolute concentration of glutamate, and baseline tissue levels of glutamate cannot be calibrated *in vivo*. Based on a previous microdialysis study reporting a baseline glutamate concentration of 0.17 μM in the ARC [24], we suspect that the absolute concentration of MBH glutamate is very small compared with the increase that is observed during feeding. Despite these limitations, we feel that the biosensor method employed herein compares favorably with microdialysis and other approaches, based on the much finer temporal resolution and real-time data acquisition it makes possible.

5. CONCLUSION

We offer the first direct evidence that in freely behaving rats, feeding is associated with rapid release of glutamate in the MBH, and that the magnitude of this release is substantially higher with HFD than chow feeding. While our findings address a key question raised by recent reports implicating MBH glutamate in the control of food intake, they also raise new questions regarding the neuronal source of MBH glutamate, the mechanisms linking its release to food consumption, the neuron populations it activates, and its consequences for the control of feeding behavior and energy balance. Answers to these questions will undoubtedly advance our understanding of food intake regulation and obesity pathogenesis.

ACKNOWLEDGMENTS

This work was supported by a National Institutes of Health (NIH) Fellowship Training Program Award (T32DK007247), an NIH National Research Service Award (F32DK091989) to S.G., the NIH-funded University of Washington Nutrition Obesity Research Center (P30 DK035816) and Diabetes Research Center (P30 DK017047), and NIH Grants DK090320, DK083042, and DK052989 to M.S.. Loan Nguyen and Alex Cubelo provided valuable technical assistance.

CONFLICT OF INTEREST

None declared.

REFERENCES

[1] Guyenet, S.J., and Schwartz, M.W., 2012. Regulation of food intake, energy balance, and body fat mass: implications for the pathogenesis and treatment of obesity. Journal of Clinical Endocrinology and Metabolism 97 (3), 745–755.

[2] Saper, C.B., Chou, T.C., and Elmquist, J.K., 2002. The need to feed: homeostatic and hedonic control of eating. Neuron 36 (2), 199–211.

[3] Kiss, J., Csaba, Z., Csaki, A., and Halasz, B., 2005. Glutamatergic innervation of neuropeptide Y and pro-opiomelanocortin-containing neurons in the hypothalamic arcuate nucleus of the rat. European Journal of Neuroscience 21 (8), 2111–2119.

[4] Martin, L.J., Blackstone, C.D., Levey, A.I., Huganir, R.L., and Price, D.L., 1993. AMPA glutamate receptor subunits are differentially distributed in rat brain. Neuroscience 53 (2), 327–358.

[5] Pinto, S., Roseberry, A.G., Liu, H., Diano, S., Shanabrough, M., and Cai, X., 2004. Rapid rewiring of arcuate nucleus feeding circuits by leptin. Science 304 (5667), 110–115.

[6] van den Pol, A.N., Wuarin, J.P., and Dudek, F.E., 1990. Glutamate, the dominant excitatory transmitter in neuroendocrine regulation. Science 250 (4985), 1276–1278.

[7] DeFalco, J., Tomishima, M., Liu, H., Zhao, C., Cai, X., Marth, J.D., and Cai, X., 2001. Virus-assisted mapping of neural inputs to a feeding center in the hypothalamus. Science 291 (5513), 2608–2613.

[8] Fahrbach, S.E., Morrell, J.I., and Pfaff, D.W., 1989. Studies of ventromedial hypothalamic afferents in the rat using three methods of HRP application. Experimental Brain Research 77 (2), 221–233.

[9] Magoul, R., Dubourg, P., Benjelloun, W., and Tramu, G., 1993. Direct and indirect enkephalinergic synaptic inputs to the rat arcuate nucleus studied by combination of retrograde tracing and immunocytochemistry. Neuroscience 55 (4), 1055–1066.

[10] Sternson, S.M., Shepherd, G.M., and Friedman, J.M., 2005. Topographic mapping of VMH –> arcuate nucleus microcircuits and their reorganization by fasting. Nature Neuroscience 8 (10), 1356–1363.

[11] Belousov, A.B., and van den Pol, A.N., 1997. Local synaptic release of glutamate from neurons in the rat hypothalamic arcuate nucleus. Journal of Physiology 499 (Pt 3), 747–761.

[12] Stanley, B.G., Ha, L.H., Spears, L.C., and Dee, M.G., 2nd, 1993. Lateral hypothalamic injections of glutamate, kainic acid, D,L-alpha-amino-3-hydroxy-5-methyl-isoxazole propionic acid or N-methyl-D-aspartic acid rapidly elicit intense transient eating in rats. Brain Research 613 (1), 88–95.

[13] Rada, P., et al., 1997. Extracellular glutamate increases in the lateral hypothalamus and decreases in the nucleus accumbens during feeding. Brain Research 768 (1–2), 338–340.

[14] Thongkhao-on, K., Wirtshafter, D., and Shippy, S.A., 2008. Feeding specific glutamate surge in the rat lateral hypothalamus revealed by low-flow push-pull perfusion. Pharmacology Biochemistry & Behavior 89 (4), 591–597.

[15] Yang, Y., et al., 2011. Hunger states switch a flip–flop memory circuit via a synaptic AMPK-dependent positive feedback loop. Cell 146 (6), 992–1003.

[16] Liu, T., Kong, D., Shah, B.P., Ye, C., Koda, S., and Saunders, A., 2012. Fasting activation of AgRP neurons requires NMDA receptors and involves spinogenesis and increased excitatory tone. Neuron 73 (3), 511–522.

[17] Tong, Q., Ye, C., McCrimmon, R.J., Dhillon, H., Choi, B., and Kramer, M.D., 2007. Synaptic glutamate release by ventromedial hypothalamic neurons is part of the neurocircuitry that prevents hypoglycemia. Cell Metabolism 5 (5), 383–393.

[18] Razolli, D.S., Solon, C., Roman, E.A., Ignacio-Souza, L.M., and Velloso, L.A., 2012. Hypothalamic action of glutamate leads to body mass reduction through a mechanism partially dependent on JAK2. Journal of Cellular Biochemistry 113 (4), 1182–1189.

[19] Shu, I.W., Lindenberg, D.L., Mizuno, T.M., Roberts, J.L., and Mobbs, C.V., 2003. The fatty acid synthase inhibitor cerulenin and feeding, like leptin, activate hypothalamic pro-opiomelanocortin (POMC) neurons. Brain Research 985 (1), 1–12.

[20] Zheng, H., Corkern, M., Stoyanova, I., Patterson, L.M., Tian, R., and Berthoud, H.R., 2003. Peptides that regulate food intake: appetite-inducing accumbens manipulation activates hypothalamic orexin neurons and inhibits POMC neurons. American Journal of Physiology—Regulatory, Integrative and Comparative Physiology 284 (6), R1436–R1444.

[21] Levin, B.E., and Dunn-Meynell, A.A., 2002. Defense of body weight depends on dietary composition and palatability in rats with diet-induced obesity. American Journal of Physiology—Regulatory, Integrative and Comparative Physiology 282 (1), R46–R54.

[22] Cabanac, M., and Rabe, E.F., 1976. Influence of a monotonous food on body weight regulation in humans. Physiology & Behavior 17 (4), 675–678.

[23] King, B.M., 2006. The rise, fall, and resurrection of the ventromedial hypothalamus in the regulation of feeding behavior and body weight. Physiology & Behavior 87 (2), 221–244.

[24] Bogdanov, M.B., Tjurmina, O.A., and Wurtman, R.J., 1996. Consumption of a high dietary dose of monosodium glutamate fails to affect extracellular glutamate levels in the hypothalamic arcuate nucleus of adult rats. Brain Research 736 (1–2), 76–81.

